the plant journal

SEB Society for Experimental Biology

The Plant Journal (2017) **91,** 361–370 doi: 10.1111/tpj.13582

RESOURCE

Sequencing and functional validation of the JGI *Brachypodium distachyon* T-DNA collection

Mon Mandy Hsia[1], Ronan O'Malley[2,3], Amy Cartwright[1,3], Rita Nieu[1], Sean P. Gordon[3], Sandra Kelly[4], Tina G. Williams[1], Delilah F. Wood[1], Yunjun Zhao[5], Jennifer Bragg[1], Mark Jordan[4], Markus Pauly[5,†], Joseph R. Ecker[2], Yong Gu[1] and John P. Vogel[1,3,5,*]

[1]*USDA ARS Western Regional Research Center, 800 Buchanan St., Albany, CA 94710-1105, USA,*
[2]*Genomic Analysis Laboratory, The Salk Institute for Biological Studies and the Howard Hughes Medical Institute, 10010 North Torrey Pines Rd., La Jolla, CA 92037, USA,*
[3]*DOE Joint Genome Institute, 2800 Mitchell Dr., Walnut Creek, CA 94598, USA,*
[4]*Cereal Research Centre, Agriculture and Agri-Food Canada, 101 Route 100, Unit 100, Morden, MB, R6M 1Y5 Canada, and*
[5]*Department of Plant and Microbial Biology, University of California, 111 Koshland Hall, Berkeley, CA 94720, USA*

Received 12 January 2017; revised 13 April 2017; accepted 18 April 2017; published online 22 April 2017.
*For correspondence (e-mail jpvogel@lbl.gov).
[†]Present address: Department of Plant Cell Biology and Biotechnology, Heinrich-Heine University, Düsseldorf, Germany.

SUMMARY

Due to a large and growing collection of genomic and experimental resources, *Brachypodium distachyon* has emerged as a powerful experimental model for the grasses. To add to these resources we sequenced 21 165 T-DNA lines, 15 569 of which were produced in this study. This increased the number of unique insertion sites in the T-DNA collection by 21 078, bringing the overall total to 26 112. Thirty-seven per cent (9754) of these insertion sites are within genes (including untranslated regions and introns) and 28% (7217) are within 500 bp of a gene. Approximately 31% of the genes in the v.2.1 annotation have been tagged in this population. To demonstrate the utility of this collection, we phenotypically characterized six T-DNA lines with insertions in genes previously shown in other systems to be involved in cellulose biosynthesis, hemicellulose biosynthesis, secondary cell wall development, DNA damage repair, wax biosynthesis and chloroplast synthesis. In all cases, the phenotypes observed supported previous studies, demonstrating the utility of this collection for plant functional genomics. The *Brachypodium* T-DNA collection can be accessed at http://jgi.doe.gov/our-science/science-programs/plant-genomics/brachypodium/brachypodium-t-dna-collection/.

Keywords: insertional mutagenesis, *Brachypodium distachyon*, functional genomics, T-DNA, mutant sequencing, model grass.

INTRODUCTION

Grasses account for the majority of calories consumed by humans, either directly as grains or indirectly through grass/grain fed animals, and are increasingly utilized for the production of sustainable biofuels. Due to population growth and increasing living standards in the developing world it is projected that crop yield must increase by 70–100% by 2050 (Editorial, 2010). Further complicating matters, these increases must occur despite loss of cropland due to degradation and urbanization. In the 1990s breeding efforts increased corn yield by only 0.78% annually (Kucharik and Ramankutty, 2005). Yield gains and breeding investments in most other crops are generally smaller than in corn. This is particularly true for the grasses being developed as biomass crops (e.g. switchgrass and *Miscanthus*), in large part due to complex genetics and the need to characterize lines over multiple years in dense stands. Thus, business as usual will not increase yield fast enough to meet projected demands. The use of basic knowledge about plant biology to design rational strategies for crop improvement is one way to accelerate crop improvement.

The use of tractable model systems and a large collaborative research community that openly shares resources and information is an efficient approach to generate this knowledge. *Arabidopsis thaliana* is the pre-eminent model plant and tremendous insights into how plants work have been made since its widespread adoption as a model system. However, as a eudicot, Arabidopsis is not suitable for studying unique areas of grass biology, including development (Glémin and Bataillon, 2009), seed biology (Olsen *et al.*, 1999) and cell wall composition (Vogel, 2008). For example, enzymes involved in synthesizing grass-specific wall structural features could not have been studied in Arabidopsis (Liu *et al.*, 2016). Indeed, even when the biology of grasses and Arabidopsis overlaps, the roles of the genes involved and their regulation can differ dramatically. For example, while flowering time and vernalization are phenotypically similar in dicots and grasses, the genes involved and their regulation differ greatly (Ream *et al.*, 2014). Thus, a truly tractable grass model system is needed and *Brachypodium distachyon* has emerged to fill this need (Brkljacic *et al.*, 2011).

Insertional mutants are a powerful tool for both forward and reverse genetics. Arabidopsis researchers have amassed a huge collection of sequence-indexed T-DNA mutants, including many homozygous mutants, that have been used extensively by the research community (O'Malley *et al.*, 2015). Similarly, a large collection of rice insertional mutants has been created by several groups (Lo *et al.*, 2016). Since rice is a valuable crop, access to these mutant resources is often limited by quarantine restrictions, intellectual property restrictions and limits on the number of lines that can be ordered each year. In an effort to develop a mutant resource for *B. distachyon* researchers, we initiated a project to create *B. distachyon* T-DNA lines. Our first set of 7145 sequence-indexed T-DNA mutants was published in 2012 (Bragg *et al.*, 2012). An additional collection of 5000 lines (1000 of which were sequenced) was created by researchers at the John Innes Centre, but unfortunately that collection is not currently accessible (Thole *et al.*, 2010).

In addition to creating knockout mutants, T-DNA insertions can also be used to overexpress nearby genes by including a transcriptional enhancer element in the T-DNA. This 'activation tagging' approach has been applied to several plant species (Hayashi *et al.*, 1992; Neff *et al.*, 1999; Weigel *et al.*, 2000; Qu *et al.*, 2008; Fladung and Polak, 2012; Carter *et al.*, 2013). Activation tagging is particularly useful for studying functionally redundant genes and essential genes where knockout mutants would lack a phenotype or would be lethal. In addition, activation tagging of genes that influence regulatory pathways could provide insight into the function of the entire pathway. The power of activation tagging is illustrated by analysis of the YUCCA genes in Arabidopsis. Since these auxin biosynthetic genes are functionally redundant, loss of function mutants cannot be identified using traditional mutant screens (Cheng *et al.*, 2006). However, by screening an activation-tagged mutant population, researchers identified two mutants with phenotypes consistent with auxin overproduction (Zhao *et al.*, 2001). In this study we greatly expand the *B. distachyon* T-DNA collection and characterize six mutants to demonstrate the utility of the collection.

RESULTS

Creation and sequencing of T-DNA lines

Transformation is the rate-limiting step in the creation of T-DNA lines. We streamlined our transformation protocol by eliminating one subculture step, which reduced labor and materials by about 20% (Bragg *et al.*, 2015). Using this improved method we created 15 409 new T-DNA lines, bringing the total *B. distachyon* T-DNA collection to 23 649 lines.

We sequenced the DNA flanking the insertion sites in 23 156 T-DNA lines using a method based on Illumina sequencing (O'Malley *et al.*, 2007). This included 1991 lines previously sequenced by Sanger sequencing (Bragg *et al.*, 2012). We identified 22 429 unique insertion sites to bring the total number of unique insertions sites in the T-DNA collection to 26 112 (Table 1, Data S2 in the Supporting Information). For 14 975 of the insertions sites we were able to assign the insertion to a single T-DNA line using the unique combination of four DNA pools containing DNA from each line (Table 1). However, for 7454 of the insertion sites we could only assign the insertion to pools of two to ten lines because the flanking sequence was not found in one of the four pools or was found in five pools due to sampling or other errors (Table 1).

We determined the location of the insertions sites with respect to genes using the JGI v.2.1 annotation (v.2.1 can

Table 1 Distribution of insertion sites

	No. of unique insertions[a]	Unique gene insertions[b]
Exon	3769	3401
Intron	3427	2622
5′-UTR	1446	1107
3′-UTR	1112	799
Near[c]	7217	4911
Intergenic	9141	na
Total	26 112	12 840

UTR, untranslated region.
[a]Tandem insertions within 500 bp were counted as one insertion.
[b]Only one insertion was counted per gene. When multiple lines had insertions in the same gene, only the most useful insertions was counted (e.g. If there was an insertion in an exon and in an intron only the insertion in the exon was counted).
[c]Insertions within 1000 bp upstream or downstream of a gene (introns, exons and UTRs).

be downloaded from the archived version 10 of Phytozome accessible through the download menu on the *B. distachyon* species page: http://phytozome.jgi.doe.gov/pz/portal.html#!info?alias=Org_Bdistachyon). Significantly, 6023 genes contain insertions in exons or introns and are thus likely to disrupt gene function. Another 1107 genes had insertions in the 5′-untranslated region (UTR) which may disrupt gene function. Thus, while this population is not saturated, 22% of the genes in the v.2.1 annotation contain insertions in exons, introns or 5′-UTRs. Data S2 contains a complete list of all insertion sites, their relative positions with respect to genes, possible Arabidopsis and rice orthologs as well as PFAM, Panther, KOG, KEGG and Gene Ontology (GO) terms. In addition, the insertion locations can be viewed on a jbrowse track in Phytozome where the insertion sites have been mapped to the v.3.1 annotation (http://phytozome.jgi.doe.gov).

Validation of the collection

We used PCR to validate the insertion site predictions for several lines from each batch of lines sequenced. The success rate for insertion sites assigned to a single T-DNA line was 98% for the second and third batches of sequenced lines and 64% for the first batch (Table 2). The lower success rate for the first batch is probably attributable to sampling error, since multiple segregating plants had to be sampled for each line due to the segregation of the transgene in the T_1 and T_2 generations. The success rate for lines assigned to pools of 10 T-DNA lines was 58% for all batches.

We used the activation tagging vector pJJ2LBA to create the T-DNA lines (Bragg *et al.*, 2012). To test the function of the 4 × 35S enhancer found on the pJJ2LBA T-DNA, we used qRT-PCR to examine the expression of genes near the insertion site in three T-DNA mutants. In each case expression of a nearby gene was increased two- to tenfold in duplicate experiments, indicating that the enhancer worked as expected (Figure S1). Given that the collection contains, on average, one T-DNA insertion every 10 kb and the enhancer can enhance expression up to at least 12 kb away (Weigel *et al.*, 2000; Qu *et al.*, 2008) the majority of *B. distachyon* genes are potential targets for activation tagging.

Phenotypic analysis to demonstrate application of insertional mutants

The ultimate demonstration of the utility of the collection is the verification and phenotypic characterization of mutants. Thus, we characterized six mutants with insertions in genes predicted to result in visible phenotypes based on prior work in other plant systems. The selected phenotypes affect cell wall composition, cell division, wax deposition or chloroplast biogenesis. For all mutants homozygous individuals were identified in the T_2 or T_3 generation using PCR. In all cases, the phenotype was recessive and co-segregated with the T-DNA insertion.

BdCESA8, a cellulose synthase

The cellulose synthase gene family is responsible for the biosynthesis of cellulose, the most important polymer in plant cell walls. In both rice and Arabidopsis, *cesa* mutants are often short, have a collapsed stem and are sometimes sterile (Turner and Somerville, 1997; Zhang *et al.*, 2009). *BdCESA8* (*Bradi2g49912*) is orthologous to *CESA8* (*At4G18780*) in Arabidopsis, which has been shown to be required for the synthesis of cellulose in secondary cell walls (Endler and Persson, 2011). Homozygous *bdcesa8* mutants (JJ18282) are shorter than the wild type and are sterile and tend to fall over (Figure 1). In addition, microscopic examination of toluidine blue-stained cross sections revealed irregularly shaped xylem cells, another hallmark of cellulose biosynthetic mutants (Figure 1c). In addition to our phenotypic analysis, the JJ18282 mutant was recently complemented with a wild-type version of Bradi2g49912, indicating that the observed phenotype is due to the mutation in Bradi2g49912 (Petrik *et al.*, 2016).

BdCSLF6, a glucosyltransferease required for mixed linkage glucan synthesis

Unlike dicots such as Arabidopsis, grasses contain the non-cellulosic glucan polymer mixed-linkage glucan (MLG) (Vogel, 2008). Members of the *Cellulose Synthase-Like*

Table 2 Verification of insertion sites

	Batch 1[a]			Batches 2 and 3		
Mutant assignment	Total no. of insertions	Insertion sites tested	Insertion sites verified (%)	Total no. of insertions	Insertion sites tested	Insertion sites verified (%)
Unique[b]	3670	42	27 (64)	11 305	104	102 (98)
Pool[c]	4430	12	7 (58)	3024	12	7 (58)

[a]Batch 1 consisted of segregating plants sampled at the T_1 or T_2 generation. Plants in batches 2 and 3 were sampled at the T_0 generation.
[b]Insertion sites were assigned to a unique T-DNA line when we obtained a given sequence in exactly four DNA pools.
[c]For sequences that only matched three DNA pools or more than four DNA pools we assigned the insertion site to a pool of 2–10 T-DNA lines.

Published 2017. This article is a U.S. Government work and is in the public domain in the USA.,
The Plant Journal, (2017), **91**, 361–370

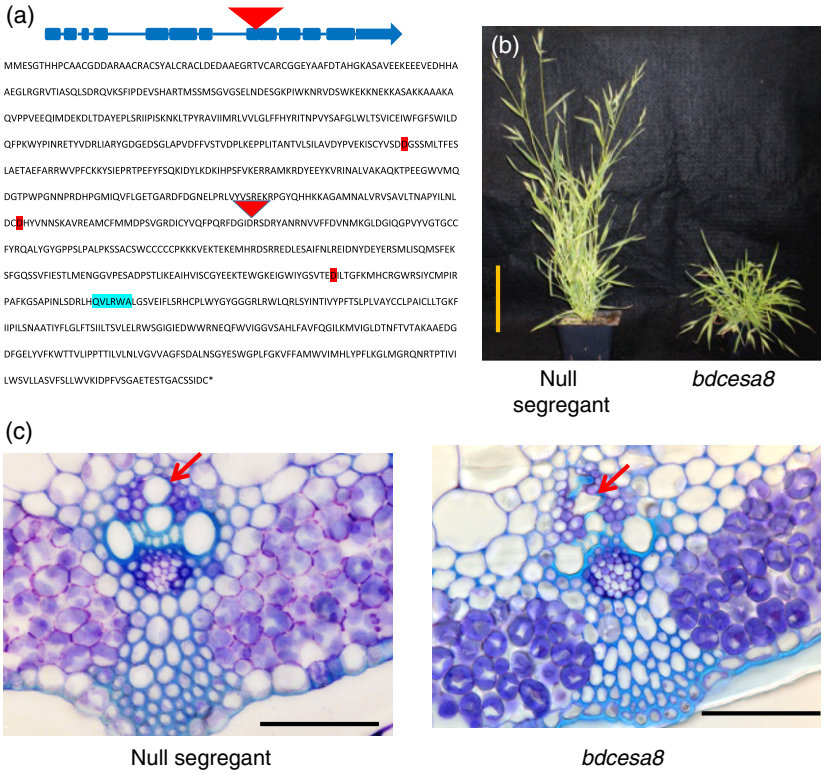

Figure 1. Phenotypic analysis of *bdcesa8*.
(a) T-DNA line JJ18282 contains an insertion in an exon of *Bradi2g49912* (inverted red triangle) within a conserved glycosol transferase domain that contains three aspartic acid residues (D, in red) and the QxxRW motif (QVLRWA, highlighted in blue).
(b) Images of 8-week-old *bdcesa8* and a null segregant sibling. Scale bar 8 cm.
(c) Cross sections of mutant and null segregant stems stained with toluidine blue. Orange arrows point to xylem cells. Note the irregular shape of the xylem cells in *bdcesa8*. Scale bar = 50 μm.

F (*CSLF*) family of glycosyltransferases are responsible for the biosynthesis of this polymer (Burton *et al.*, 2006; Schreiber *et al.*, 2014). Overexpression of a barley CslF (HvCslF6) lead to a three- to fourfold increase of MLGs in leaves (Burton *et al.*, 2011). In contrast, homozygous mutants of rice *CSLF6* (MSU ID LOC_Os08g06380; RAP ID Os08g0160500) are short and have a reduced MLG content (Vega-Sanchez *et al.*, 2012). We identified a T-DNA insertion in *BdCSLF6* (*Bradi3g16307*) the *B. distachyon* ortholog of the rice *CSLF6* (Figure 2a). We observed a similar growth phenotype and decreased MLG content in the *bdcslf6* mutant, indicating that *BdCSLF6* represents a MLG synthase (Figure 2b, c).

Mutations in *BdWAT1* lead to an irregular cell shape

Cell wall development is a complex process involving many genes in addition to those that synthesize the major structural polymers. The gene *walls are thin 1* (*WAT1*) encodes a tonoplast protein that is required for normal formation of secondary cell wall. It was first identified as a gene whose expression correlated with secondary cell wall biosynthesis in *in vitro* xylogenic culture of zinnia (*Zinna elegans*) (Pesquet *et al.*, 2005). An Arabidopsis mutant, *wat1-1*, with a T-DNA insertion in the gene orthologous to zinnia *WAT1* is dwarf with irregularly shaped epidermal cells (Ranocha *et al.*, 2010). The *wat1-1* mutant also has severely decreased secondary cell wall thickening of interfascicular and xylary fibers (Ranocha *et al.*, 2010). We identified a mutant, JJ24902, with an insertion in the orthologous *B. distachyon* gene, *Bradi1g21860* (*BdWAT1*). Similar to the Arabidopsis mutant, *bdwat1* plants were dwarf, developmentally delayed and had irregularly shaped xylem (Figure 3).

BdRAD51, a gene required for male and female sterility

RAD51C is important for meiosis in both ovule and pollen development, but has no effect on mitosis in somatic tissue (Abe *et al.*, 2005). Arabidopsis *rad51c* mutants appear vegetatively wild type but are defective in both ovule and pollen development (Abe *et al.*, 2005). We identified a *B. distachyon* mutant JJCRC377 in the orthologous gene *Bradi2g41710* (*BdRAD51C*). Like the Arabidopsis *rad51c* mutant, *bdrad51c* plants were vegetatively wild type but completely sterile (Figure 4). *bdrad51c* pollen appeared shrunken and deformed and did not stain with Alexander's viability stain (Figure 4c).

BdWAX2, a gene required for cuticular wax biosynthesis

The *WAX2* gene has been shown to be required for deposition of leaf cuticular wax in Arabidopsis, rice and maize (Aarts *et al.*, 1995; Sturaro *et al.*, 2005; Qin *et al.*, 2011). Arabidopsis *wax2* mutants have glossy, bright green leaves due to decreased cuticular wax (Aarts *et al.*, 1995). Rice and maize *wax2* mutants also have decreased leaf cuticular wax, but leaf color in them is unchanged (Sturaro *et al.*, 2005; Qin *et al.*, 2011). In these species the most

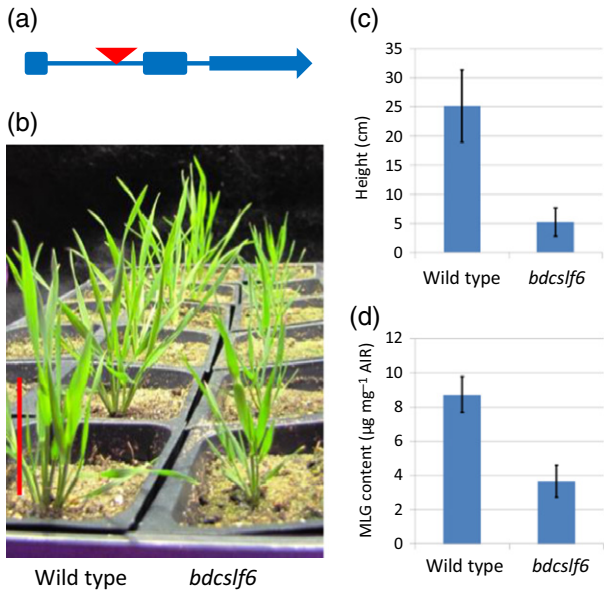

Figure 2. Phenotypic analysis of *bdcslf6*.
(a) Graphical representation of the T-DNA insertion in the first intron of *Bradi3g1630*.
(b) Visual appearance of 3-week-old seedlings. Scale bar = 4 cm.
(c) Average height of 2-week-old plants ±SD ($n = 6$, $P < 10^{-6}$).
(d) Mixed-linkage glucan (MLG) content in 8-day-old seedlings. Four biological and three technical replicates were performed ($n = 12$, $P < 0.01$ for Student's *t*-test).

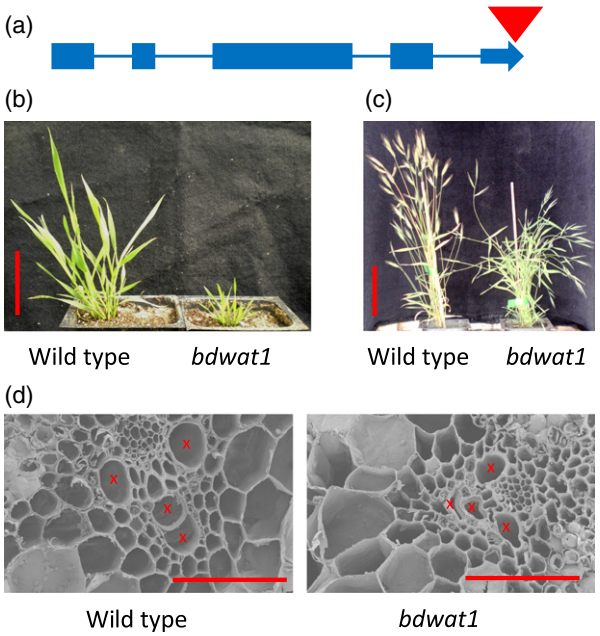

Figure 3. Phenotypic analysis of *bdwat1*.
(a) Illustration of the T-DNA insertion site in line JJ24092 in *Bradi1g21860* (*BdWAT1*).
(b). Appearance of 3-week-old plants. Note the dwarf phenotype of *bdwat1*. Scale bar = 4 cm.
(c) Appearance of 8-week-old adult plants. Note the drooping stems, and that, though delayed, *bdwat1* eventually flowers and makes seed. Scale bar = 8 cm.
(d) Scanning electron micrographs of stem cross sections. Xylem cells are denoted by a red 'x'. Note the irregularly shaped cells in *bdwat1*. Scale bars = 50 µm.

obvious phenotype is a loss of leaf hydrophobicity when water drops are placed on the leaf surface. We identified a T-DNA line, JJ17731, in the orthologous *B. distachyon* gene *Bradi3g48997* (*BdWAX2*). As expected, the plants had decreased cuticular wax and a loss of hydrophobicity (Figure 5). Leaf color was unchanged, as was observed in maize and rice.

BdTAB2, a gene required for proper chloroplast function

Chloroplast function is dependent upon the translation of genes coded by the chloroplast genome. The *TAB2* (translation of *psaB* mRNA) gene is a nuclear gene required for the translation of the chloroplast *psaB* mRNA that codes for a polypeptide required for the function of photosystem I; it was first identified in the unicellular green alga *Chlamydomonas* (Dauvillee *et al.*, 2003). The *TAB2* gene family is ancient and conserved among prokaryotes and eukaryotes that perform oxygenic photosynthesis. (Dauvillee *et al.*, 2003). Mutations in three of the Arabidopsis *ATAB2* orthologs result in albino plants with abnormal chloroplasts due to a lack of PsaB protein (Barneche *et al.*, 2006). We identified a *B. distachyon* mutant, JJ24116, with an insertion in the *B. distachyon TAB2* orthlog, *Bradi3g48480*. *bdtab2* mutants are yellow, like Arabidopsis *atab2* mutants, and die shortly after germination, presumably due to lack of functional chloroplasts (Figure 6).

DISCUSSION

We used optimized methods to create and sequence T-DNA lines to gain significant savings of time, cost and labor without compromising accuracy. We streamlined the transformation procedure by decreasing the time the callus is under selection and eliminating an entire subculture. This reduced the time required to generate transgenic lines, reduced the labor required by a quarter and deceased the materials required. These improvements enabled us to generate about 14 000 T_1 lines within 15 months or about 900–1000 lines per month. This translates to about 100 lines per week per person working full time on transformation or only 0.8 h of labor per line.

We evaluated the quality of the data in several ways. First, we used PCR to determine the accuracy of insertion site predictions. A remarkable 98% of the insertions assigned to a single line produced in this study were verified. To demonstrate the utility of the collection we phenotypically characterized six lines with mutations in genes previously shown to have obvious phenotypes in other species. In each case, the phenotype observed in the *B. distachyon* mutant was consistent with observations in

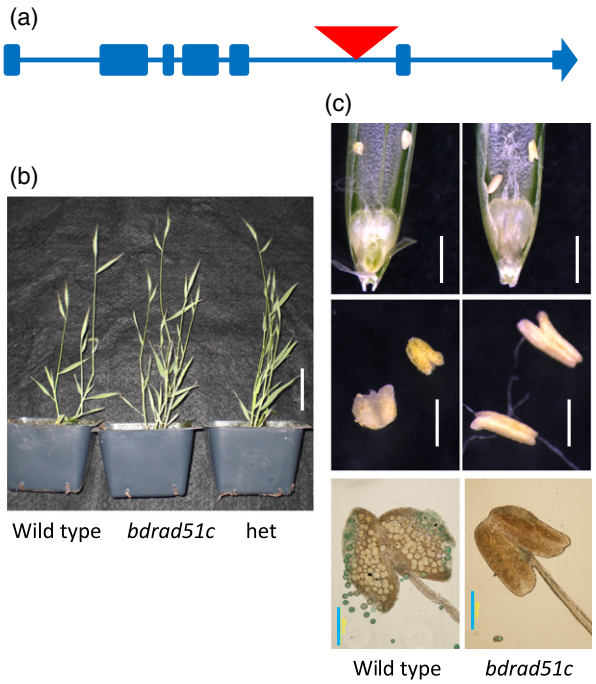

Figure 4. Phenotypic analysis of *bdrad51c*.
(a) Illustration of the T-DNA insertion site in line CRC377. Note that the T-DNA has inserted into an intron in gene *Bradi2g41710* (*BdRAD51c*).
(b) Images of 4-week-old hemizygous, homozygous mutant and wild-type plants. Note that *bdrad51c* plants have a wild-type appearance. Scale bar = 4 cm.
(c) *bdrad51c* plants are male sterile. Top panel: dissected flowers showing shrunken anthers in *bdrad51c*. Scale bar = 1 mm. Middle panel: anthers. Scale bar = 1 mm. Bottom panel: anthers stained with Alexander's stain. Viable pollen stains blue. Scale bar = 200 μm.

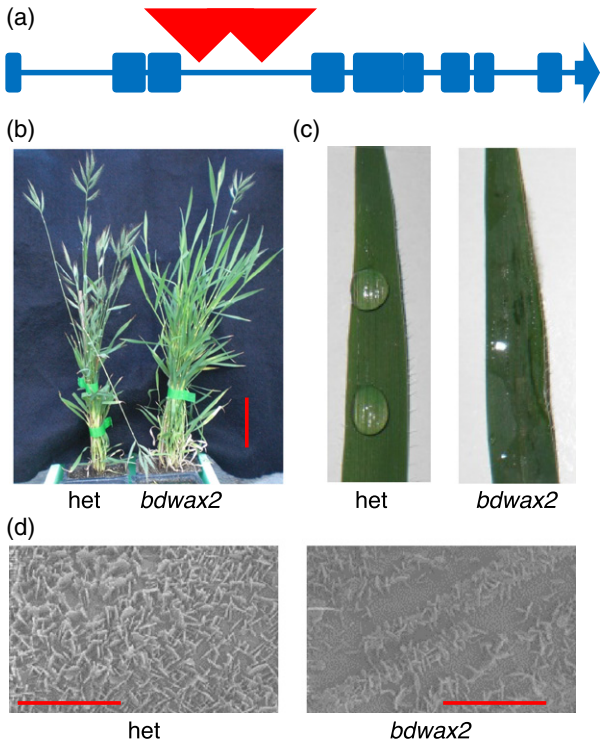

Figure 5. Phenotypic analysis of *bdwax2*.
(a) Illustration of the tandem T-DNA insertion sites in line JJ17731 into *Bradi3g48997* (*BdWAX2*).
(b) Images of 5-week-old heterozygous and *bdwax2* plants. Scale bar = 8 cm. Heterozygous plants have a wild-type appearance.
(c) Images of water droplets on heterozygous and *bdwax2* leaves. Note that water does not bead on *bdwax2* due to decreased wax and hydrophobicity.
(d) Scanning electron micrographs of heterozygous and *bdwax2* leaves. Note that *bdwax2* leaves have fewer wax crystals. Scale bar = 50 μm.

other species. This validates every step in the process from the creation of the lines to the assignment of insertion sites to specific genes. We also showed that the enhancer element found in the pJJ2LBA construct was correlated with overexpression of nearby genes, indicating that the population can be used for activation tagging.

The sequence indexed T-DNA lines produced by this project are a valuable resource for the plant science community, and is already heavily utilized. Indeed, we have already filled 270 seed requests for 10 252 lines (Figure 7). Instructions for ordering mutants and updates to the mutant table found in File S1 can be found on the T-DNA project website http://jgi.doe.gov/our-science/science-programs/plant-genomics/brachypodium/brachypodium-t-dna-collection/. In addition, the T-DNA insertion sites are included as a jbrowse track in Phytozome, as described in Figure 7(c).

EXPERIMENTAL PROCEDURES

Production of T-DNA lines and plant growth conditions

Line Bd21-3 was used for all experiments (Vogel and Hill, 2008). Plants were grown as described (Bragg *et al.*, 2015). *Agrobacterium* tumefaciens mediated transformation was performed as described (Bragg *et al.*, 2015). The activation tagging vector pJJ2LBA was used for all transformations (Bragg *et al.*, 2012).

Tissue sampling and DNA extraction

Leaf samples (5–8 cm) from each individual mutant were placed into a unique combination of four pools. Since the first batch of mutants consisted of T_1 or T_2 plants segregating for the T-DNA inserts, we planted 10–12 seeds for each line and placed leaf samples from three plants into each assigned pool. Later batches consisted entirely of T_0 plants so leaf samples were simply placed into the assigned pools. DNA was extracted from the pooled leaves.

DNA extraction and retrieval of the T-DNA flanking sequence

DNA was extracted using a cetyltrimethylammonium bromide (CTAB) extraction method modified from Murray and Thompson (1980). Pooled leaf samples were ground into a fine powder using a mortar and pestle. Twenty milliliters of extraction buffer [2% CTAB (Fisher Scientific, O3042-500, https://www.fishersci.com/), 100 mM Trizma base pH 9.5 (Sigma, 99349, http://www.sigmaaldrich.com/), 1.4 M NaCl (Fisher Scientific, S271-3), 1% PEG 6000 (Fisher Scientific, AC192280010), 20 mM EDTA (Fisher

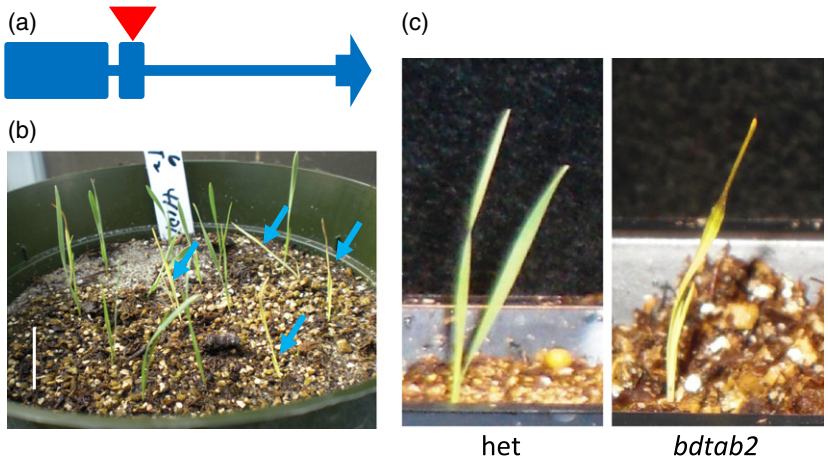

Figure 6. Phenotype of *bdtab2*.
(a) Illustration of *BdTAB2* T-DNA insertion in line JJ24116 into an exon of *Bradi3g48460* (*BdTAB2*).
(b) Segregating T_1 plants of line JJ24116. Arrows point toward seedlings homozygous for the T-DNA insertion. Scale bar is 3 cm.
(c) Close-up images of 1-week-old heterozygous and homozygous sibling plants.

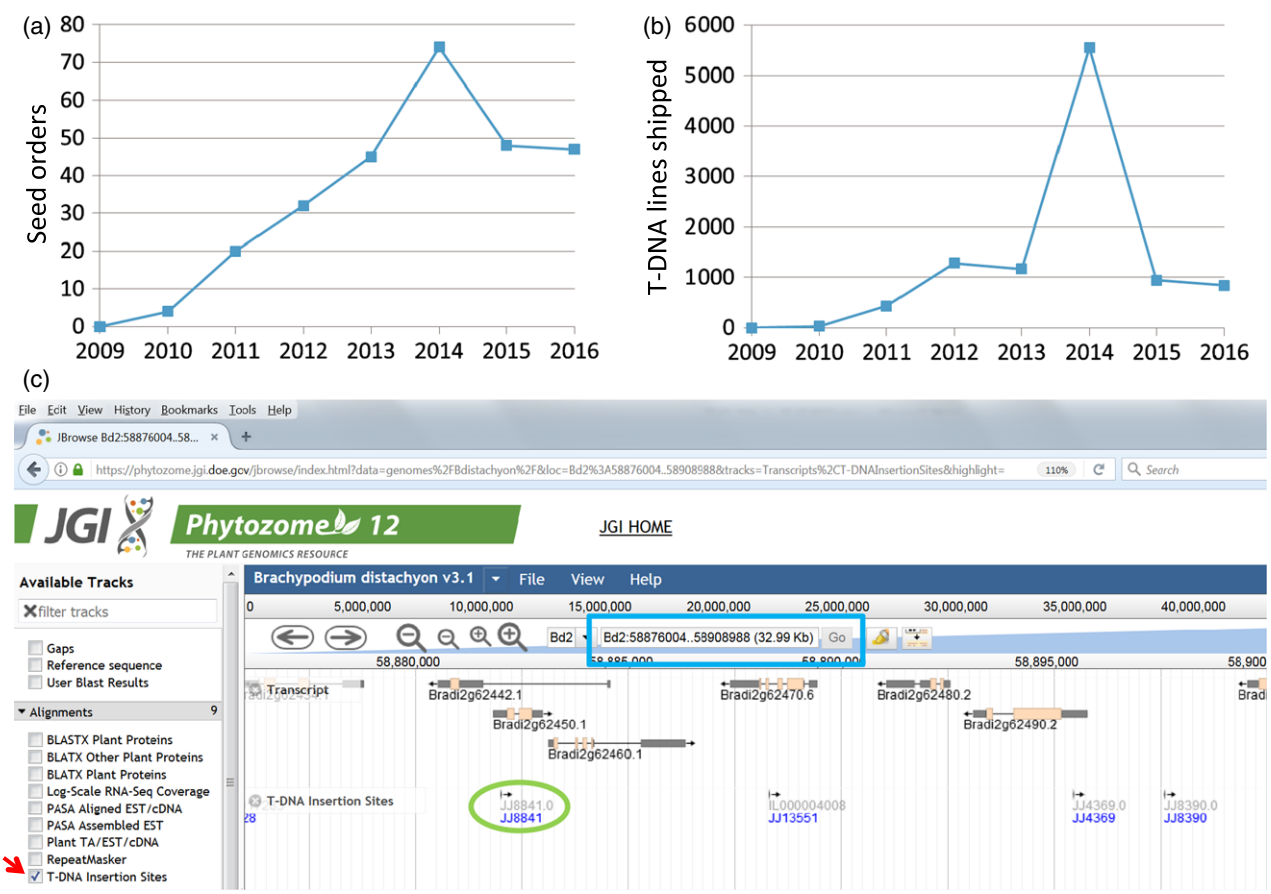

Figure 7. T-DNA seed distribution and database.
(a) Number of seed requests.
(b) Number of lines shipped. Note the spike in demand when the lines described in this paper became available.
(c) Screenshot from the Phytozome database showing locations of T-DNA insertions. To display the T-DNA insertion track simply check the 'T-DNA insert sites' box indicated by the red arrow on the left. Gene models are indicated on the top track. Other tracks can be displayed by checking the boxes on the left. The search box highlighted by the blue rectangle can be used to search for T-DNA lines, insertion sites or genes. One T-DNA insertion is highlighted by the green oval. The grey text on the top indicates the name of the insertion site and the blue text below indicates the name of the T-DNA line containing that insertion.

Published 2017. This article is a U.S. Government work and is in the public domain in the USA.,
The Plant Journal, (2017), **91**, 361–370

Scientific, BP120-1), 2% polyvinylpyrrolidone (Fisher Scientific, 9003-39-8) and 0.25% mercaptoethanol (Fisher Scientific, BP176-100)] were added to 5 ml of leaf powder. Samples were vortex briefly at maximum speed to mix and incubated at 65°C for 1 h. An equal volume of phenol–chloroform:isoamyl alcohol, pH 6.7 (25:24:1, Fisher Scientific, BP17521-400) was then added and mixed by gently inverting the tube before spinning at 7000 ***g*** at room temperature (22°C) for 10 min. The aqueous phase was transferred to a new tube and an equal volume of chloroform: isoamyl alcohol (24:1, Fisher Scientific, AC32715-5000) was added. Tubes were gently inverted before centrifugation at 7000 ***g*** at room temperature for 10 min. The aqueous phase was transferred to a new tube and 0.7 volumes of isopropanol at room temperature was added before centrifugation at 7000 ***g*** at room temperature for 10 min. The supernatant was discarded without disturbing the pellet. The pellet was washed with 70% ethanol and centrifuged at 7000 ***g*** at room temperature for 5 min. The supernatant was discarded and the pellet air dried overnight. DNA was resuspended in 200–500 μl of 1× TE (10 mM Tris, 1 mM EDTA pH 8.0). RNA was digested by the addition of 10 μg ml^{-1} RNaseA (Life Technologies, EN0531, https://www.thermofisher.com/uk/en/home/brands/life-technologies.html) by incubating at 37°C for 1 h and then overnight at 4°C. DNA flanking the insertion sites was sequenced using a high-throughput sequencing and data analysis pipeline based on an adapter ligation method (O'Malley *et al.*, 2007) using the primers listed in Table S1.

Insertion site characterization

T-DNA insertions were mapped to the reference genome (v.2.1, http://phytozome.jgi.doe.gov/pz/portal.html). Genomic features were extracted from the phytozome v.2.1 annotation using custom perl scripts and their position was intersected with genomic features using BedTools (version 2.20.1). After our analysis, the insertion sites were transferred to the v.3.0 genome assembly by BLAT alignment of 1000 bp of flanking sequence on either side of the insertion site.

PCR genotyping

Small leaf samples were collected and placed in extraction buffer following the manufacturer's protocol (Thermo Scientific Phire Plant Direct PCR Kit #F-130WH, https://www.thermofisher.com/). PCR using gene-specific primers both alone and with left border T-DNA primer T3, approximately 120 bp into the left border, using the Phire kit PCR protocol and samples were analyzed on 1% agarose gel to the determine genotype (see Data S1 for genotyping primers and instructions).

Mixed-linkage glucan measurement

Seeds were stratified at 4°C for 1 week, then grown in a growth chamber with 20 h daylight, 70% relative humidity, 24°C and 4 h darkness, 70% relative humidity, 18°C. Seedlings were harvested and freeze dried 8 days after germination. Alcohol insoluble reside (AIR) was prepared as described (Foster *et al.*, 2010) and the MLG content was determined using the corresponding Megazyme kit (Megazyme, https://www.megazyme.com/). Briefly, AIR was digested with lichenase, which releases specific oligosaccharides that are then digested to glucose by a β-glucosidase. The released glucose was then quantified colorimetrically using glucose oxidase and peroxidase (McCleary and Codd, 1991). The assay was adapted to the manufacturer's instructions for small-scale preparations (5 mg AIR) by dividing all reaction volumes by 10.

Microscopy

For low-temperature scanning electron microscopy (cryo SEM) of leaf cuticle wax, fresh leaves were cut and mounted onto a copper sample holder with Tissue-Tek adhesive (Sakura Finetek USA Inc., http://www.sakura-americas.com/) and then prepared for cryo SEM using an Alto 2500 cryo system (Gatan Inc., http://www.gatan.com/). The sample holder containing the adherent sample was attached to the rod of a vacuum transfer device and plunged into liquid nitrogen slush. After freezing, the holder and sample were pulled up into the vacuum transfer device and transferred under vacuum to the cryo preparation stage. The holder and sample were heated to −85°C for 20 min to remove ice from the sample surface. The sample and holder were chilled back to −180°C and sputter coated with gold–palladium inside the cryo preparation chamber. The holder and sample were transferred to the SEM cryo stage, where the temperature did not exceed −135°C, for observation and photography.

For *bdwat1* we performed ambient SEM of the stem tissue as well. Stem tissues were cut into 1 cm lengths and placed directly into a vial containing a fixative consisting of 2% formaldehyde, 2.5% glutaraldehyde and 2.5 mM calcium chloride in 0.1 M sodium cacodylate buffer, pH 6.9 for at least 24 h for fixation. Samples were rinsed in 0.1 M sodium cacodylate buffer three times (20 min per rinse), dehydrated in an ethanol graded series and critical point dried in a Tousimis Autosamdri 815 (Tousimis, http://www.tousimis.com/). The specimens were then mounted onto aluminum specimen stubs using double adhesive coated carbon tabs (Ted Pella, Inc., http://www.tedpella.com/). All SEM samples were viewed and photographed in a Hitachi S-4700 field emission scanning electron microscope (Hitachi, http://www.hitachi.com/) at 2 kV. Images were captured at a pixel resolution of 2560 × 1920.

bdcesa8 and *bdwat1* stem section images were prepared for light microscopy by cutting the stems into pieces 5 mm long and fixing in the above fixative for a minimum of 24 h. The stem tissues were dehydrated in an ethanol–butanol graded series (Jensen, 1962), infiltrated and embedded in glycol methacrylate (Technovit 7100, Heraeus Kulzer GmbH, http://kulzer.com/, imported by Electron Microsocopy Sciences, https://www.emsdiasum.com/microscopy/) according to the manufacturer's instructions. The resulting polymerized block was sectioned into 5 μm thick cross and longitudinal sections. Sections were stained in 0.05% toludine blue for 2 min and mounted in water. Pollen viability was tested by staining 4-week-old anthers in Alexander's stain (Alexander, 1969) for 5 min at room temperature, then washing and mounting in water. All samples were viewed and photographed using bright-field conditions in a Leica DM4000B compound microscope (Leica Microsystems, http://www.leica-microsystems.com/).

ACCESSION NUMBERS

Bradi2g49912, Bradi3g16307, Bradi1g21860, Bradi2g41710, Bradi3g48997 and Bradi3g48480.

ACKNOWLEDGEMENTS

We would like to thank David Goodstein and Richard Hayes for incorporating the data into Phytozome, Leila Hornick for creating the JGI Brachypodium webpages and David Hantz and Julie Calfas for plant care. Funding was provided by Office of Biological and Environmental Research, Office of Science, US Department of Energy, interagency agreements DE-SC0001526 and DE-AI02-07ER64452. The work conducted by the US Department of Energy

Joint Genome Institute, a DOE Office of Science User Facility, is supported under contract no. DE-AC02-05CH11231. This work was also supported by grants from the National Science Foundation (MCB 0726408 and 1122250) to JRE and by the Office of Science (BER), US Department of Energy, grant no DE-SC0012400 to YZ and MP.

CONFLICT OF INTEREST

The authors declare no conflict of interest.

SUPPORTING INFORMATION

Additional Supporting Information may be found in the online version of this article.

Figure S1. An example of activation tagging.

Table S1. List of the sequencing primers used.

Data S1. Detailed genotyping instructions and explanatory figures.

Data S2. A list of all T-DNA insertion sites along with the genes affected, annotations and other details.

REFERENCES

Aarts, M.G., Keijzer, C.J., Stiekema, W.J. and Pereira, A. (1995) Molecular characterization of the CER1 gene of arabidopsis involved in epicuticular wax biosynthesis and pollen fertility. *Plant Cell*, **7**, 2115–2127.

Abe, K., Osakabe, K., Nakayama, S., Endo, M., Tagiri, A., Todoriki, S., Ichikawa, H. and Toki, S. (2005) Arabidopsis RAD51C gene is important for homologous recombination in meiosis and mitosis. *Plant Physiol.* **139**, 896–908.

Alexander, M.P. (1969) Differential staining of aborted and nonaborted pollen. *Biotech. Histochem.* **44**, 117–122.

Barneche, F., Winter, V., Crevecoeur, M. and Rochaix, J.D. (2006) ATAB2 is a novel factor in the signalling pathway of light-controlled synthesis of photosystem proteins. *EMBO J.* **25**, 5907–5918.

Bragg, J.N., Wu, J., Gordon, S.P., Guttman, M.E., Thilmony, R., Lazo, G.R., Gu, Y.Q. and Vogel, J.P. (2012) Generation and characterization of the Western Regional Research Center Brachypodium T-DNA insertional mutant collection. *PLoS One*, **7**, e41916.

Bragg, J.N., Anderton, A., Nieu, R. and Vogel, J.P. (2015) Brachypodium distachyon. *Methods Mol. Biol.* 17–33.

Brkljacic, J., Grotewold, E., Scholl, S. *et al.* (2011) Brachypodium as a model for the grasses: today and the future. *Plant Physiol.* **157**, 3–13.

Burton, R.A., Collins, H.M., Kibble, N.A.J., *et al.* (2011) Over-expression of specific HvCslF cellulose synthase-like genes in transgenic barley increases the levels of cell wall (1,3;1,4)-β-d-glucans and alters their fine structure. *Plant Biotechnol J.*, **9**, 117–135.

Burton, R.A., Wilson, S.M., Hrmova, M., Harvey, A.J., Shirley, N.J., Medhurst, A., Stone, B.A., Newbigin, E.J., Bacic, A. and Fincher, G.B. (2006) Cellulose synthase-like CslF genes mediate the synthesis of cell wall (1,3;1,4)-?-D-glucans. *Science*, **311**, 1940–1942.

Carter, J.D., Pereira, A., Dickerman, A.W. and Veilleux, R.E. (2013) An active ac/ds transposon system for activation tagging in tomato cultivar m82 using clonal propagation. *Plant Physiol.* **162**, 145–156.

Cheng, Y., Dai, X. and Zhao, Y. (2006) Auxin biosynthesis by the YUCCA flavin monooxygenases controls the formation of floral organs and vascular tissues in Arabidopsis. *Genes Dev.* **20**, 1790–1799.

Dauvillee, D., Stampacchia, O., Girard-Bascou, J. and Rochaix, J.D. (2003) Tab2 is a novel conserved RNA binding protein required for translation of the chloroplast psaB mRNA. *EMBO J.* **22**, 6378–6388.

Editorial. (2010) How to feed a hungry world. *Nature*, **466**, 531–532.

Endler, A. and Persson, S. (2011) Cellulose synthases and synthesis in Arabidopsis. *Mol. Plant*, **4**, 199–211.

Fladung, M. and Polak, O. (2012) Ac/Ds-transposon activation tagging in poplar: a powerful tool for gene discovery. *BMC Genom.* **13**, 61.

Foster, C.E., Martin, T.M. and Pauly, M. (2010) *Comprehensive compositional analysis of plant cell walls (lignocellulosic biomass) part II: carbohydrates*. Exp: J. Vis e1837. https://doi.org/10.3791/1837.

Glémin, S. and Bataillon, T. (2009) A comparative view of the evolution of grasses under domestication: tansley review. *New Phytol.* **183**, 273–290.

Hayashi, H., Czaja, I., Lubenow, H., Schell, J. and Walden, R. (1992) Activation of a plant gene by T-DNA tagging: auxin-independent growth *in vitro*. *Science*, **258**, 1350–1353.

Jensen, W.A. (1962) *Histological Procedures, Tissue Infiltration and Paraffin Infiltration. In Botanical Histochemistry: Principles and Practice*. San Francisco: W.H. Freeman and Company, pp. 62–64; 80–81.

Kucharik, C.J. and Ramankutty, N. (2005) Trends and variability in U.S. Corn yields over the twentieth century. *Earth Interact.* **9**, 1–29.

Liu, L., Hsia, M.M., Dama, M., Vogel, J. and Pauly, M. (2016) A xyloglucan backbone 6-O-acetyltransferase from Brachypodium distachyon modulates xyloglucan xylosylation. *Mol. Plant*, **9**, 615–617.

Lo, S.F., Fan, M.J., Hsing, Y.I. *et al.* (2016) Genetic resources offer efficient tools for rice functional genomics research. *Plant Cell Environ.* **39**, 998–1013.

McCleary, B.V. and Codd, R. (1991) Measurement of (1→3), (1→4)-ß-D-Glucan in Barley and Oats: A Streamlined Enzymic Procedure. *J. Sci. Food. Agric.*, **55**, 303–312.

Murray, M.G. and Thompson, W.F. (1980) Rapid isolation of high molecular weight plant DNA. *Nucleic Acids Res.* **8**, 4321–4326.

Neff, M.M., Nguyen, S.M., Malancharuvil, E.J. *et al.* (1999) BAS1: a gene regulating brassinosteroid levels and light responsiveness in Arabidopsis. *Proc. Natl Acad. Sci. USA*, **96**, 15316–15323.

Olsen, O.A., Linnestad, C. and Nichols, S.E. (1999) Developmental biology of the cereal endosperm. *Trends Plant Sci.* **4**, 253–257.

O'Malley, R.C., Alonso, J.M., Kim, C.J., Leisse, T.J. and Ecker, J.R. (2007) An adapter ligation-mediated PCR method for high-throughput mapping of T-DNA inserts in the Arabidopsis genome. *Nat. Protoc.* **2**, 2910–2917.

O'Malley, R.C., Barragan, C.C. and Ecker, J.R. (2015) A user's guide to the arabidopsis T-DNA insertion mutant collections. *Methods Mol. Biol.* 323–342.

Pesquet, E., Ranocha, P., Legay, S., Digonnet, C., Barbier, O., Pichon, M. and Goffner, D. (2005) Novel markers of xylogenesis in zinnia are differentially regulated by auxin and cytokinin. *Plant Physiol.* **139**, 1821–1839.

Petrik, D.L., Cass, C.L., Padmakshan, D., Foster, C.E., Vogel, J.P., Karlen, S.D., Ralph, J. and Sedbrook, J.C. (2016) BdCESA7, BdCESA8, and BdPMT utility promoter constructs for targeted expression to secondary cell-wall-forming cells of grasses. *Front. Plant Sci.***7**, 1–4.

Qin, B.X., Tang, D., Huang, J. *et al.* (2011) Rice OsGL1-1 is involved in leaf cuticular wax and cuticle membrane. *Mol. Plant*, **4**, 985–995.

Qu, S., Desai, A., Wing, R. and Sundaresan, V. (2008) A versatile transposon-based activation tag vector system for functional genomics in cereals and other monocot plants. *Plant Physiol.* **146**, 189–199.

Ranocha, P., Denance, N., Vanholme, R. *et al.* (2010) Walls are thin 1 (WAT1), an Arabidopsis homolog of Medicago truncatula NODULIN21, is a tonoplast-localized protein required for secondary wall formation in fibers. *Plant J.* **63**, 469–483.

Ream, T.S., Woods, D.P., Schwartz, C.J., Sanabria, C.P., Mahoy, J.A., Walters, E.M., Kaeppler, H.F. and Amasino, R.M. (2014) Interaction of photoperiod and vernalization determines flowering time of Brachypodium distachyon. *Plant Physiol.* **164**, 694–709.

Schreiber, M., Wright, F., MacKenzie, K. *et al.* (2014) The barley genome sequence assembly reveals three additional members of the CslF (1,3;1,4)-β-glucan synthase gene family. *PLoS One*, **9**, 1–9.

Sturaro, M., Hartings, H., Schmelzer, E., Velasco, R., Salamini, F. and Motto, M. (2005) Cloning and characterization of GLOSSY1, a maize gene involved in cuticle membrane and wax production. *Plant Physiol.* **138**, 478–489.

Thole, V., Worland, B., Wright, J., Bevan, M.W. and Vain, P. (2010) Distribution and characterization of more than 1000 T-DNA tags in the genome of *Brachypodium distachyon* community standard line Bd21. *Plant Biotechnol. J.* **8**, 734–747.

Turner, S.R. and Somerville, C.R. (1997) Collapsed xylem phenotype of Arabidopsis identifies mutants deficient in cellulose deposition in the secondary cell wall. *Plant Cell*, **9**, 689–701.

Vega-Sanchez, M.E., Verhertbruggen, Y., Christensen, U. *et al.* (2012) Loss of cellulose synthase-like F6 function affects mixed-linkage glucan deposition, cell wall mechanical properties, and defense responses in vegetative tissues of rice. *Plant Physiol.* **159**, 56–69.

Vogel, J. (2008) Unique aspects of the grass cell wall. *Curr. Opin. Plant Biol.* **11**, 301–307.

Vogel, J. and Hill, T. (2008) High-efficiency *Agrobacterium*-mediated transformation of *Brachypodium distachyon* inbred line Bd21-3. *Plant Cell Rep.* **27**, 471–478.

Weigel, D., Ahn, J.H., Blazquez, M.A. *et al.* (2000) Activation tagging in Arabidopsis. *Plant Physiol.* **122**, 1003–1013.

Zhang, B., Deng, L., Qian, Q., Xiong, G., Zeng, D., Li, R., Guo, L., Li, J. and Zhou, Y. (2009) A missense mutation in the transmembrane domain of CESA4 affects protein abundance in the plasma membrane and results in abnormal cell wall biosynthesis in rice. *Plant Mol. Biol.* **71**, 509–524.

Zhao, Y., Christensen, S.K., Fankhauser, C., Cashman, J.R., Cohen, J.D., Weigel, D. and Chory, J. (2001) A role for flavin monooxygenase-like enzymes in auxin biosynthesis. *Science*, **291**, 306–309.